TUNABLE RESONATOR ARRAYS – TRANSMISSION, NEAR-FIELD INTERACTIONS AND EFFECTIVE PROPERTY EXTRACTION

D .Smirnov Salford University
O. Umnova Salford University

1 INTRODUCTION

The slotted cylinder (SC) acting as a Helmholtz resonator is used as the fundamental building block of the resonator arrays investigated in this paper. Similar arrays using SCs have been studied in noise control applications [1] and as acoustic metamaterial elements [2]. Here analytic, semi-analytic and numerical models are presented and compared with the goal of studying the near-field interactions of two coupled SCs in isolation and within an array consisting of unit cells of two SCs. The double SC cell facilitates tuning by rotating the two SCs, allowing the coupling to be changed and thus affecting the macroscopic characteristic of the array.

A scattering model and resonance frequency calculation is presented by Lagarrigue et al. [1] for a single SC (using the term 'split ring') and a single SC facing a rigid boundary, the latter case being equivalent to two SCs radiating in phase with the boundary replaced by a mirror line. The results presented in this paper follow a methodology similar to the one used in this past work, however the effect of simplifications and approximations have been thoroughly investigated to create new optimised scattering and resonance frequency calculation models which yield closer matches to results obtained using finite-element modelling (FEM).

Analytic solutions for wave scattering by a single SC, two SCs, and an infinite row of SC pairs are first described in Section 2. Aside from an approximation prohibiting circumferentially travelling waves in the slot treating the air inside it as a piston, these solutions are exact and when truncated and evaluated numerically yield close matches to FEM results produced using COMSOL 4.3. In Section 3, low frequency approximations are applied to the scattering model, yielding simple expressions which characterise the resonance frequencies, including a model of the SC as a damped mass-spring system. Finally, an improved homogenisation method based on the effective fluid layer concept presented by Fokin et al [5] is described in Section 4 and used to predict the behaviour of an arbitrary number of rows using results from only one row.

2 SCATTERED WAVE SOLUTIONS

2.1 General Solution and Slotted Cylinder in Isolation

The general analytic solution in terms of wavenumber k using the $e^{-i\omega t}$ time-harmonic convention is obtained by solving the Helmholtz equation in cylindrical coordinates in 3 domains – outside the cylinder, inside and in the slot, then matching the eigenfunction expansions across the boundaries. The cylinders are considered as infinitely tall, neglecting the z dimension and reducing the problem to 2D polar coordinates (r, θ). Only the monopole terms are permitted inside the slot, and average pressure obtained using integration across the slot is used for matching, treating the air in the slot as a piston. The walls of the cylinder are treated as perfectly rigid, using Neumann boundary conditions.

Figure 1 illustrates the SC geometry, and pressure in the 3 aforementioned domains is defined in (1). The terms r_i and r_o describe the inner radius, ψ descirbes the slot opening angle in radians and θ_s describes the slot orientation (clockwise rotation from facing $\theta = 0$ in the coordinate system). $J_n(\dots)$ and $H_n(\dots)$ represent Bessel functions and Hankel functions of the first kind respectively, with the notation $H_n^*(\dots)$ used for Hankel functions of the second kind; here n is the order term.

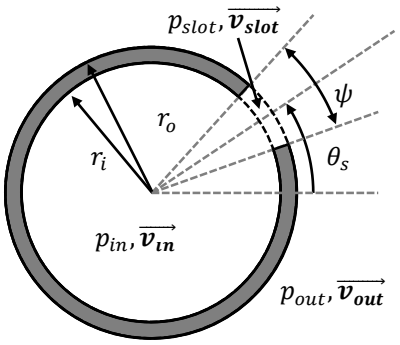

Figure 1: Slotted cylinder geometry

The scattered wave formulation is used in the external domain – the scattering coefficients B_n are unknown, and the coefficients E_n represent the external field incident onto the SC – to generalise the solution these are either known and represent a source or can be unknown and include waves scattered by other nearby cylinders.

$$p = \begin{cases} p_{out} = \sum_{n\in\mathbb{Z}} \big(B_n H_n(kr) + E_n J_n(kr)\big) e^{in\theta}, & r > r_o \\ p_{slot} = D\big(H_0(kr) + R_s H_0^*(kr)\big), & r_i \le r \le r_o, \theta_s - \psi/2 \le \theta \le \theta_s + \psi/2 \\ p_{in} = \sum_{n\in\mathbb{Z}} A_n J_n(kr) e^{in\theta}, & r < r_o \end{cases} \quad (1)$$

The coefficents A_n, D and R_s depend only on the cylinder interior and are eliminated, and the solution for B_n in terms of E_n is:

$$B_n = -E_n \frac{J_n'(kr_o)}{H_n'(kr_o)} + \Psi_n e^{-in\theta_s} \sum_{m\in\mathbb{Z}} E_m \frac{\operatorname{sinc}\left(\frac{m\psi}{2}\right)}{H_m'(kr_o)} e^{im\theta_s} \quad (2)$$

The terms $\Psi_n = \psi \operatorname{sinc}(n\psi/2)/i\pi^2 kr_o H_n'(kr_o)\widetilde{Z_t}$ feature in their denominator the total lumped impedance $\overline{Z_t}$ defined in (3) which is experienced by the air 'piston' in the slot when forced by the external field, in the normalised form $\widetilde{Z_t} = \overline{Z_t}/\, i\rho_0 c_0$ where ρ_0 and c_0 are the air density and sound speed in the external medum. $\overline{Z_t}$ consists of the averaged radiation impedance $\overline{Z_r}$ minus the impedance looking into the slot $\overline{Z_s}$, the latter in turn depending on the impedance averaged of the inner cavity $\overline{Z_c}$. R_s is the reflection coefficient relating waves travelling into and out of the cylinder, and as the cylinder is lossless $|R_s| = 1$:

$$\overline{Z_t} = \overline{Z_r} - \overline{Z_s}, \qquad \overline{Z_r} = i\rho_0 c_0 \frac{\psi}{2\pi} \sum_{n\in\mathbb{Z}} \frac{H_n(kr_o)}{H_n'(kr_o)} \operatorname{sinc}\left(\frac{n\psi}{2}\right)^2, \qquad \overline{Z_s} = i\rho_o c_o \frac{H_0(kr_o) + R_s H_0^*(kr_o)}{H_1(kr_o) + R_s H_1^*(kr_o)} \quad (3)$$

$$R_s = -\frac{H_0(kr_i) + \widetilde{Z_c} H_1(kr_i)}{H_0^*(kr_i) + \widetilde{Z_c} H_1^*(kr_i)}, \qquad i\rho_0 c_0 \widetilde{Z_c} = \overline{Z_c} = i\rho_0 c_0 \frac{\psi}{2\pi} \sum_{n\in\mathbb{Z}} \frac{J_n(kr_i)}{J_n'(kr_i)} \operatorname{sinc}\left(\frac{n\psi}{2}\right)^2 \quad (4)$$

To solve for scattering of a plane wave by a single SC, the Jacobi-Anger expansion [3] can be used to specify an incident plane wave with incidence angle θ_{inc}, resulting in the substitution $E_n = i^n e^{-in\theta_{inc}}$.

2.2 Multiple Scattering Solutions

Multiple scattering solutions for more than one cylinder are readily obtained from the form in (2) by substituting forms of external field coefficients E_n which feature incident source terms S_n as well as terms describing the field scattered by other cylinders expressed at the origin of the cylinder in question. Each cylinder has its own coordinate system with the origin at its centre, and the expansions are equated using Graf's addition theorem [3].

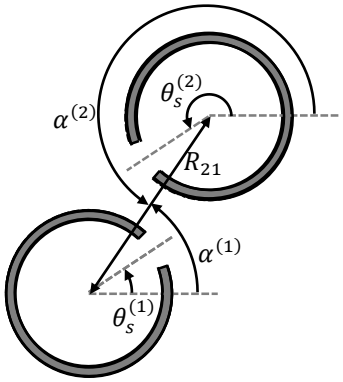

Figure 2: SC pair orientation

2.2.1 Slotted Cylinder Pair

For a pair of identical SCs at arbitrary orientation (illustrated in Figure 2) stimulated by an incident source represented by coefficients S_n, the field external to each cylinder incorporates terms resulting from the field scattered by the other cylinder. Adopting the superscripted notation $(\ldots)^{(1,2)}$ to mean that terms for either cylinder 1 or 2 should be substituted as required, the coefficients for the field external to each cylinder are:

$$E_n^{(1,2)} = I^{(1,2)} S_n + \sum_{m\in\mathbb{Z}} B_m^{(2,1)} L_{m-n}^{(1,2)}, \qquad L_n^{(1,2)} = H_n(kR_{21}) e^{in\alpha^{(2,1)}} \tag{5}$$

The terms $I^{(1,2)}$ account for the change in value of the incident field due to offset of each cylinder from the origin – for a plane wave, this is just a phase offset; R_{21} is the distance between the cylinder centres, $\alpha^{(1)}$ is the angle at which the origin of cylinder 2 is seen from the origin of the cylinder 1 and $\alpha^{(2)}$ is the converse. The expressions for $B_n^{(1,2)}$ are then obtained by substituting form of (5) for each cylinder into (2), results can be evaluated numerically by truncating the infinite system of equations to limit $|n|$:

$$\begin{aligned} B_n^{(1,2)} + \frac{J_n'(kr_o)}{H_n'(kr_o)} \sum_{m\in\mathbb{Z}} B_m^{(2,1)} \left(L_{m-n}^{(1,2)} - \Psi_n e^{-in\theta_{s,1}} \sum_{q\in\mathbb{Z}} L_{m-q}^{(1,2)} \frac{\operatorname{sinc}\left(\frac{q\psi}{2}\right)}{H_q'(kr_o)} e^{iq\theta_s^{(1,2)}} \right) \\ = I^{(1,2)} \left(\Psi_n e^{-in\theta_s^{(1,2)}} \sum_{m\in\mathbb{Z}} S_m \frac{\operatorname{sinc}\left(\frac{m\psi}{2}\right)}{H_m'(kr_o)} e^{im\theta_s^{(1,2)}} - S_n \frac{J_n'(kr_o)}{H_n'(kr_o)} \right) \end{aligned} \tag{6}$$

2.2.2 Infinite Row of Slotted Cylinder Pairs

The behaviour of an infinite row consisting of identical cells of two SCs (see Figure 5 for an example cell) can be determined by solving for the scattering coefficients for the two cylinders in just one cell – provided that the incident field is a plane wave then the waves scattered by the remaining cells can be recovered by multiplying by a phase factor corresponding to the phase shift in the incident plane wave at the cell with respect to the original cell.

$$\begin{aligned} B_n^{(1,2)} + \sum_{m\in\mathbb{Z}} B_m^{(1,2)} \left(P_{m-n} \frac{J_n'(kr_o)}{H_n'(kr_o)} - \Psi_n e^{-in\theta_s^{(1,2)}} \sum_{q\in\mathbb{Z}} B_m P_{m-q} \frac{\operatorname{sinc}\left(\frac{q\psi}{2}\right)}{H_q'(kr_o)} e^{iq\theta_s^{(1,2)}} \right) \\ + \sum_{m\in\mathbb{Z}} B_m^{(2,1)} \left(\frac{J_n'(kr_o)}{H_n'(kr_o)} \mathrm{Q}_{m,n}^{(1,2)} - \Psi_n e^{-in\theta_s^{(1,2)}} \sum_{q\in\mathbb{Z}} \mathrm{Q}_{m,q}^{1} \frac{\operatorname{sinc}\left(\frac{q\psi}{2}\right)}{H_q'(kr_o)} e^{iq\theta_s^{(1,2)}} \right) \\ = I_1^{(1,2)} \left(\Psi_n e^{-in\theta_s^{(1,2)}} \sum_{m\in\mathbb{Z}} S_m \frac{\operatorname{sinc}\left(\frac{m\psi}{2}\right)}{H_m'(kr_o)} e^{im\theta_s^{(1,2)}} - S_n \frac{J_n'(kr_o)}{H_n'(kr_o)} \right) \end{aligned} \tag{7}$$

$$\mathrm{Q}_{m,n}^{(1,2)} = L_{m-n}^{(1,2)} + \sum_{q\in\mathbb{Z}} J_{q-n}(kR_{21}) P_{m-q}\, e^{i(q-n)\alpha^{(2,1)}}, \qquad P_n = \sum_{l=1}^{\infty} H_n(lkd)(I_{row}^{l} i^{-n} + I_{row}^{-l} i^{n}) \tag{8}$$

The terms P_n are a type of Schlömilch series which are slowly convergent and impractical to evaluate directly, therefore an alternative computationally efficient form of the series as given by Linton [4] is used to generate the semi-analytical results.

3 CHARACTERISATION OF RESONANCE

3.1 Slotted Cylinder as Damped Mass-Spring Model

When small-argument expansions for $J_n(\dots)$ and $H_n(\dots)$ as given by Abramowitz and Stegun [8] are substituted in the total lumped impedance $\overline{Z_t}$ assuming $kr_i, kr_o < 1$, the following form can be obtained:

$$\overline{Z_t} = \overline{Z_r} - \overline{Z_s} \approx \rho_0 \frac{\psi}{4} \omega r_o - i\rho_0 \frac{\psi}{\pi} \left(\omega r_o \left(\frac{15}{4} - 2\ln(\psi) \right) - \frac{c_0^2}{\omega r_i} \cdot \frac{r_o}{r_i} \right) \tag{9}$$

This form can be equated to the impedance of a damped mass-spring system $R_{rad} - i\omega M - K/i\omega$:

$$R_{rad} = \rho_0 \frac{\psi r_o}{4} \omega, \qquad M = \rho_o r_o \left(\frac{\psi}{\pi} \left(\frac{15}{4} - 2\ln(\psi) \right) + \frac{h}{r_i} \right), \qquad K = \frac{\rho_0 c_0^2 \psi r_o}{\pi r_i^2} \tag{10}$$

The resistive term R_{rad} can be neglected to estimate the resonance frequency (h is the wall thickness defined as $h = r_o - r_i$):

$$\omega_{res} = \sqrt{K/M} = \frac{c_0}{r_i \sqrt{\left(\frac{15}{4} - 2\ln(\psi) \right) + \frac{h}{r_i} \cdot \frac{\pi}{\psi}}} \tag{11}$$

To estimate the Q factor of the resonance, assuming the resonance is sufficiently narrow in frequency, the value of the radiation loss can be evaluated at the resonance frequency:

$$Q_{res} = \sqrt{KM} / R_{rad}|_{\omega=\omega_{res}} = \frac{4M}{\rho_0 \psi r_o} = \left(\frac{1}{\pi} (15 - 8\ln(\psi)) + \frac{4h}{r_i \psi} \right) \tag{12}$$

A comparison of the resonance wavenumber-radius product $kr_{o,res} = \omega_{res} r_o / c_0$ calculated using (12) with FEM results is shown in Figure 3 in the next section for a range of SC geometry proportions.

3.2 Resonance Frequencies of Slotted Cylinder Pair

To estimate the resonance frequencies of two interacting cylinders, the incident field is set to zero before using the small-argument expansions, solving the eigenvalue problem without forcing terms for the more complex geometry. Since absolute orientation is no longer important, the two cylinders are positioned along the x axis so that $\alpha^{(2)} = \pi$, and twisting mutual orientation is assumed so that $\theta_s^{(1)} = \pi + \theta_s^{(2)}$. The expression for radiation impedance of the first cylinder becomes:

$$\widetilde{Z_r}^{(1)} = \sum_{n \in \mathbb{Z}} \beta_n \left(\frac{H_n(kr_o)}{H_n'(kr_o)} - \frac{J_n(kr_o)}{J_n'(kr_o)} \right) \operatorname{sinc}\left(\frac{n\psi}{2} \right) + \frac{\psi}{2\pi} \sum_{n \in \mathbb{Z}} \frac{J_n(kr_o)}{J_n'(kr_o)} \operatorname{sinc}^2\left(\frac{n\psi}{2} \right) \tag{13}$$

The modified coefficients $\beta_n = B_n^{(1)} / u_1 e^{in\theta_{s,1}}$ are normalised by u_1, the velocity at the slot of cylinder 1. The in-phase and out-of-phase resonances are specifically desired, in which case the assumptions $C_n = \pm(-1)^n B_n$ and hence $\widetilde{Z_r}^{(2)} = \widetilde{Z_r}^{(1)}$ are valid. Applying small-argument expansions [8] for Bessel and Hankel functions results in the following expression for the normalised radiation impedance:

$$\widetilde{Z_r} = \frac{\psi}{2\pi} kr_o \ln(kr_o) + \frac{\psi}{\pi} kr_o \sum_{n \in \mathbb{N}^+} \frac{\operatorname{sinc}^2\left(\frac{n\psi}{2} \right)}{n} - 2kr_o G, \qquad G = \sum_{n \in \mathbb{N}^+} (\beta_n + \beta_{-n}) \frac{\operatorname{sinc}\left(\frac{n\psi}{2} \right)}{n} \tag{14}$$

For $n > 0$, the terms β_n and β_{-n} are computed using two different equations:

$$\begin{cases} \beta_n \mp \sum_{m\in\mathbb{N}^+} \beta_{-m} \frac{(n+m-1)!}{m!\,(n-1)!} \left(\frac{r_o}{R_{21}}\right)^{m+n} e^{i(n+m)\theta_{s,1}} = \frac{\psi}{2\pi}\left(\operatorname{sinc}\left(\frac{n\psi}{2}\right) \pm \frac{1}{2}\left(\frac{r_o}{R_{21}}\right)^{n} e^{in\theta_{s,1}}\right) \\ \beta_{-n} \mp \sum_{m\in\mathbb{N}^+} \beta_{m} \frac{(n+m-1)!}{m!\,(n-1)!} \left(\frac{r_o}{R_{21}}\right)^{m+n} e^{-i(n+m)\theta_{s,1}} = \frac{\psi}{2\pi}\left(\operatorname{sinc}\left(\frac{n\psi}{2}\right) \pm \frac{1}{2}\left(\frac{r_o}{R_{21}}\right)^{n} e^{-in\theta_{s,1}}\right) \end{cases} \tag{15}$$

Using the results, the radiation impedance $i\rho_0 c_0 \overline{Z_r}$ is matched to the normalized slot impedance $\overline{Z_s}$ in a similar fashion to (9), and substituting either $+$ or $-$ for $\pm$ in expressions (15) for the in-phase and out-of-phase vibration respectively, the following expression for the resonance frequency is derived:

$$\omega_{res} = \frac{c_0}{r_i\sqrt{\left(\frac{3}{4} + \frac{\pi}{\psi}\left(\frac{h}{r_i} + 2G\right)\right)}} \tag{16}$$

Figure 4 shows comparison of the resonance wavenumber-radius product $kr_{0,res} = \omega_{res} r_o / c_0$ calculated using (16) with FEM results for an SC pair with $\psi = \pi/8$, $r_i = 0.95 r_o$ and $R_{21} = 2.2 r_o$.

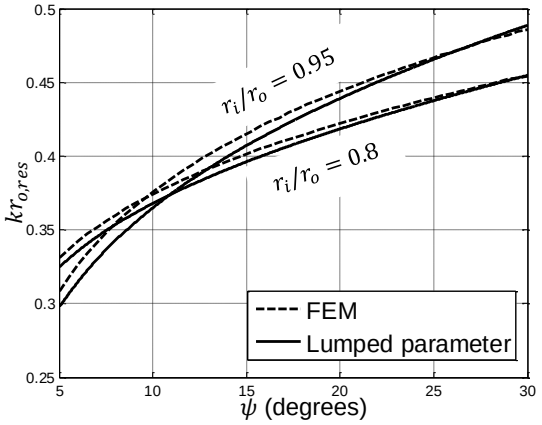

Figure 3: Single SC resonance

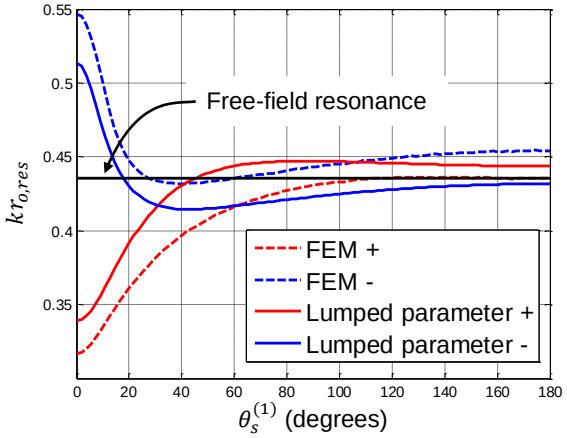

Figure 4: Double SC resonance

4 HOMOGENISATION

4.1 Reflection and Transmission of Single Row and Behaviour as Fluid Layer

At a distance from an infinite row of scatterers, the reflected and transmitted field due to a plane wave incident at angle θ_{inc} from the $+x$ direction can be represented via an expansion in Cartesian (x, y) coordinates as a superposition of plane wave modes with different components of the wavenumber along the x direction, k_x. Due to quasi-periodicity, the y components all match with the incident plane wave. By examining a general expansion of this form it can be shown that within the long wavelength limit stated in (17), there is only one propagating reflected and only one propagating transmitted mode, as all other modes have imaginary k_x values and therefore are evanescent (d_y is the size of the 'cell' or lattice constant in the y direction):

$$kd_y < \frac{2\pi}{1 + |\sin(\theta_{inc})|} \tag{17}$$

Hence, at a sufficient distance from the scatterer row so that the contributions of the evanescent waves approach zero, the row can be treated as a homogeneous layer of fluid with certain effective properties. The effective properties can be extracted using the plane wave reflection and transmission coefficients R and T of the row, and then can be used to predict the behaviour of multiple rows. R and T for an

infinite row of dual-scatterer cells can be calculated from the two sets of coefficients in (7) for each scatterer within the unit cell as:

$$R = \frac{2}{kd_y \cos(\theta_{inc})} \sum_{n\in\mathbb{Z}} i^n e^{-in\theta_{inc}} \left(\frac{B_n^{(1)}}{I_{ref}^{(1)}} + \frac{B_n^{(2)}}{I_{ref}^{(2)}} \right), \qquad T = 1 + \frac{2}{kd_y \cos(\theta_{inc})} \sum_{n\in\mathbb{Z}} i^{-n} e^{in\theta_{inc}} \left(\frac{B_n^{(1)}}{I^{(1)}} + \frac{B_n^{(2)}}{I^{(2)}} \right) \quad (18)$$

These expressions are the result of equating large-argument approximations of Hankel functions (given by Abramowitz and Stegun [8]) for scattered pressure due to a plane wave represented using Huygens' principle expressed as a continuous limit of a discrete sum of 2D point sources. The results are equivalent to those presented by Twersky [7] for a row of single-scatterer cells, with added phase factors to account for the spatial offsets of the scatterers within the cell. I_1 and I_2 are the same phase offsets related to the SC positions as in (5), (6), and (7) and I_{1R} and I_{2R} for the reflected wave are defined as:

$$I_{ref}^{(1,2)} = e^{-ik\left(x^{(1,2)}\cos(\theta_{inc}) - y^{(1,2)}\sin(\theta_{inc})\right)} \quad (19)$$

Results for R and T obtained via the semi-analytic scattering model and via FEM using COMSOL were found to be almost identical and as such a comparison is not shown here.

4.2 Effective Property Extraction

A method of effective property extraction from an infinite row of scatterers has been presented by Fokin [5]. The method used here uses the same concept but has several additions, permitting arbitrary incidence angles and asymmetric unit cells. Cells which are asymmetric around $x = 0$ cannot be equated to a fluid layer centred at $x = 0$, as this erroneously produces lossy effective wavenumber and impedance values which violate energy conservation, and these then give incorrect results when the effective properties are used to predict the behaviour of multiple infinite rows. To combat this problem, the effective fluid layer is offset from the centre position at $x = 0$ by a value which is determined from R and T to satisfy energy conservation. This uses the known result that a layer of lossless fluid causes the phase relation between the reflected and transmitted waves at equal distances on opposing sides of the layer surface to be $\pm\pi/2$, as is shown by Lekner [6]. Hence, instead of directly using R from (18), the reflection coefficient for an offset row R_{off} is used in the effective property extraction:

$$R_{off} = Re^{-2ik_0^x d_{x,off}}, \qquad k_0^x d_{x,off} = \{\arg(R/T)/2 + \pi/4 + n\pi : n \in \mathbb{Z}\} \quad (20)$$

The two effective properties of interest are the x component of the effective wavenumber k_{eff}^x and the value $\mathcal{Z}$, related to the normalised impedance of the effective fluid as $\mathcal{Z} = \rho_{eff} k_o^x / k_{eff}^x \rho_o$:

$$k_{eff}^x d_x = \left\{ i \ln\left(\frac{1/\phi^2 - \mathcal{S}R_{off}}{T} \right) + 2\pi n : n \in \mathbb{Z} \right\}, \qquad \mathcal{Z} = \pm \sqrt{\frac{\left(R_{off} + 1/\phi^2\right)^2 - T^2}{\left(R_{off} - 1/\phi^2\right)^2 - T^2}} \quad (21)$$

Here, the term ϕ is defined as $\phi = e^{ik_0^x d_x/2}$ is the phase offset experienced by the plane wave when it travels half of the row's size in the x direction, and the term $\mathcal{S}$ is the reflection coefficient of a half-space (layer of infinite width) of the medium with the effective properties, calculated as:

$$\mathcal{S} = (\mathcal{Z} - 1)/(\mathcal{Z} + 1) \quad (22)$$

4.3 Application of Effective Properties

Once the effective properties are calculated, in order to obtain reflection and transmission coefficients for a multiple number of rows, a new value of d_x is taken to match the size of the integer number of rows, and then the expressions obtained by reversing the derivation for the effective fluid layer are used to calculate the new R and T, shifting R back by the asymmetry-related phase factor:

$$R = e^{-2ik_0^x d_{x,off}} \frac{1}{\phi^2} \cdot \frac{\vartheta^2 - 1/\vartheta^2}{\mathcal{S}\vartheta^2 - 1/\mathcal{S}\vartheta^2}, \qquad T = \frac{1}{\phi^2} \cdot \frac{\mathcal{S} - 1/\mathcal{S}}{\mathcal{S}\vartheta^2 - 1/\mathcal{S}\vartheta^2} \tag{23}$$

The term $\vartheta = e^{ik_{eff}^x d_x/2}$ is the equivalent of ϕ for the effective wavenumber. Figure 5 shows a comparison of the homogenised semi-analytic results with FEM results for a two-SC unit cell with $\psi = \pi/8$, $r_i = 0.95r_o$, $R_{21} = 2.2r_o$. The SCs are distributed equidistantly from the centre of the square cell with $d_x, d_y = 5r_o$ along its diagonal. Results as a function of twisting angle $\theta_s^{(1)}$ are shown in Figure 6. The parameter $|\mathcal{S}|$ is used as a practical means of characterising large arrays.

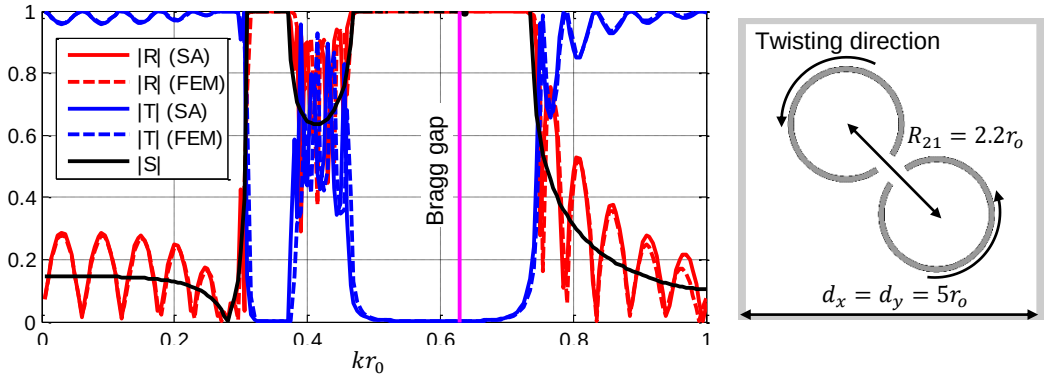

Figure 5: reflection and transmission behavior of 10 rows calculated via the homogenised semi-analytic model compared with FEM results t, with half-space reflection magnitude $|\mathcal{S}|$ overlaid

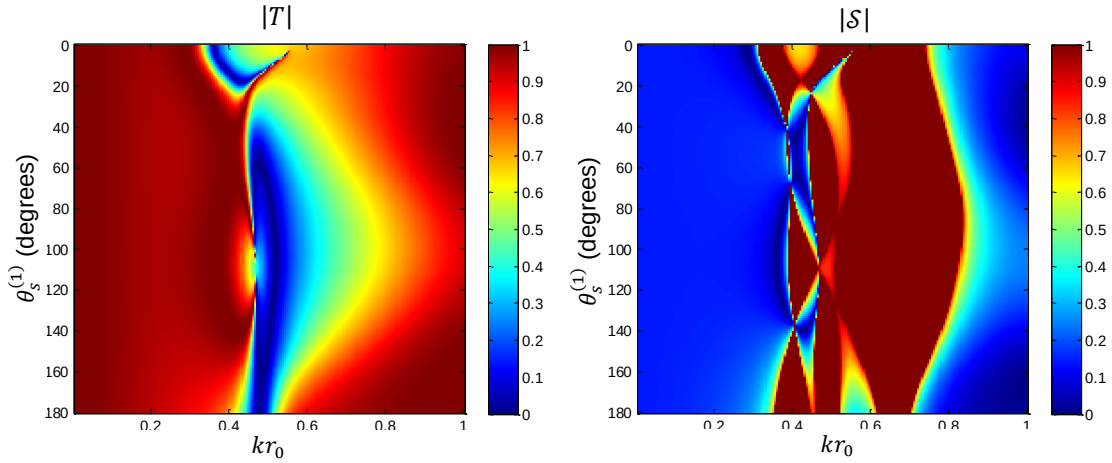

Figure 6: transmission through a single row $|T|$ and half-space reflection magnitude $|\mathcal{S}|$ for an array with the unit cell shown in Figure 5 as a function of twisting angle

5 DISCUSSION

The free-field and array results for the two interacting cylinders demonstrate the existence of two coupled resonance frequencies, a lower in-phase resonance frequency and a higher anti-phase resonance frequency. The two frequencies diverge as coupling is increased by rotating the slots towards each other. The small-argument approximations leading to expressions (15) and (16) predict the divergent behaviour which is seen in the semi-analytic and FEM scattering results, however more aggressive approximations are required to simplify the problem (for instance, the assumption $kR_{21} < 1$ is not necessarily valid) and as a result the approximate equation does not match the FEM results as closely as the results for the single cylinder, incorrectly suggesting crossing of the two resonance frequencies. Nevertheless, the approximation can serve to illustrate the SC pair behaviour.

Within the array, the behaviour of the twisted SC pair is more complicated than in free-field due to the additional loading by the nearby geometry. The effect of the splitting of the resonance frequencies is similar to the free-field case for the results for one row with sparse unit cells (e.g. $|T|$ in Figure 6) however become more complicated due to the effects of periodicity in an array (e.g. $|\mathcal{S}|$ in Figure 6). The results where $\theta_s^{(1)}$ is close to 0 agree with the findings by Cheng and Liu [2] of resonance-related transmission gaps with a 'transparency window' in between, and additionally behaviour when the mutual orientation of the SCs is modified is also observed. Many unit cell configurations are possible so it is not trivial to comprehensively characterise the behaviour of the SC pair within an array, however it is clear that the mutual orientation has a major effect on the transmission characteristics.

The derivations here are distinguished from those presented by Lagarrigue et al. [1] as the scattering model uses truncated Hankel expansion in the slot defined in (1) rather than an exponential plane wave expansion (which does not account for the curvature of the geometry) producing an improved scattering model; also the small-argument expansions do not neglect the $H_0(\ldots)$ terms, allowing a more accurate calculation of resonance frequency including of the radiation loss. Furthermore, an approximation of summations of the form $\sum_{n\in\mathbb{N}^+} \mathrm{sinc}^2(n\psi/2)\,/n$, which arise in the expansions of the impedances (incorporated into the term δ defined by Lagarrigue et al. [1] as (21) in the text) was derived, allowing the resonance frequency of one SC to be simply calculated using expression (16).

6 CONCLUSION

Tunable resonator arrays using two slotted cylinders as the unit cell were examined using a combination of semi-analytic and approximate models, the validity of which was verified using FEM results. Improved scattering, lumped parameter and homogenisation methods were proposed and applied to the problem. Tuning the resonator array by rotating the slotted cylinders was found to have a significant effect on the macroscopic transmission properties of the array by changing the coupling of the cylinder pairs.

The approximate models presented allow the calculation of the uncoupled single resonance and coupled resonance frequencies. The homogenisation method together with the approximate resonance frequency calculation provide computationally efficient tools to analyse the behaviour of the resonator array. If greater precision of the approximate models is required, then an avenue for future investigation is an improved coupled resonator model and the extension of the lumped parameter model to the array.

7 REFERENCES

1. C. Lagarrigue, J.P. Groby, V. Tournat, O. Dazel and O. Umnova., 'Absorption of sound by porous layers with embedded periodic arrays of resonant inclusions', J. Acoust. Soc. Am., 134 (6) 4670-4680. (December 2013).
2. Y. Cheng, X. Liu, 'Coupled resonant modes in twisted acoustic metamaterials', Appl. Phys. A, Vol 109, 805-811 (2012).
3. P. A. Martin. Multiple scattering: interaction of time-harmonic waves with N obstacles. University Press, 36-40 (2006).
4. C. M. Linton. Schlömilch series that arise in diffraction theory and their efficient computation. Department of Mathematical Sciences, Loughborough (2005).
5. V. Fokin, A. Muralidhar, S. Cheng and Z. Xiang, 'Method for retrieving effective properties of locally resonant acoustic metamaterials', Physical Review B, Vo. 76 144302 (October 2007).
6. J. Lekner, 'The phase relation between reflected and transmitted waves, and some consequences', Americal Journal of Physics, Vol. 58, 317-320 (1990).
7. V. Twersky, 'On scattering of waves by the infinite grating of circular cylinders', IRE Transactions of Antennas and Propagation, Vol. 10, 737-765 (1962).
8. M. Abramowitz and I. A. Stegun. Handbook of mathematical functions with formulas, graphs and mathematical tables. Dover Books, 360-364 (1970).